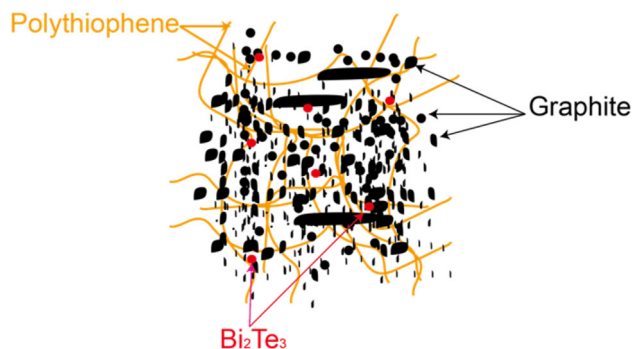


# Preparation and Characterization of Bi<sub>2</sub>Te<sub>3</sub>/Graphite/ Polythiophene Thermoelectric Composites

CHUNHUA LAI,<sup>1</sup> JUNJIE LI,<sup>1</sup> CHENGJUN PAN,<sup>1,2</sup> LEI WANG,<sup>1,3</sup>  
and XIAOJUN BAI<sup>1</sup>

1.—Shenzhen Key Laboratory of Polymer Science and Technology, College of Materials Science and Engineering, Shenzhen University, Shenzhen 518060, China. 2.—e-mail: pancj@szu.edu.cn. 3.—e-mail: wl@szu.edu.cn

The Bi<sub>2</sub>Te<sub>3</sub>/graphite/polythiophene composites were prepared by solution mixing, mechanical ball milling, cold pressing and spark plasma sintering (SPS) in order to utilize and integrate the high Seebeck coefficient of Bi<sub>2</sub>Te<sub>3</sub>, high electrical conductivity of graphite (G) and low thermal conductivity of polythiophene (PTh). The structures and properties of the composites were characterized by scanning electron microscope, thermo gravimetric analyzer, x-ray diffraction and ULVAC ZEM-2 Seebeck coefficient measurement. The results showed that the related components were uniformly dispersed in the composites, and the electrical conductivity of the composites increased significantly with increasing G content. A small addition of Bi<sub>2</sub>Te<sub>3</sub> to the matrix contributed to an increase in Seebeck coefficient and the thermal conductivity of the composites stayed at a low level owing to the low thermal conductivity of PTh. These composites prepared by SPS show an increase in Seebeck coefficient but a decrease in electrical conductivity as compared to corresponding composites prepared by cold pressing.



**Key words:** Polythiophene, Bi<sub>2</sub>Te<sub>3</sub>, composite, thermoelectric properties

## INTRODUCTION

Thermoelectric (TE) systems are promising devices for energy harvesting owing to their great potential as

energy converters between thermal and electrical energy.<sup>1,2</sup> Previous studies have generally focused on relatively high-efficiency inorganic TE materials, such as Bi<sub>2</sub>Te<sub>3</sub>, Bi-Te alloys, CoSb<sub>3</sub>, SiGe, and MgSi.<sup>3–5</sup> However, the inherent drawbacks of inorganic thermoelectric materials, including potential for heavy metal pollution, processing difficulties, and high cost, have impeded their widespread practical applications as energy materials.<sup>6</sup> In this regard, recent research

has been mostly concentrated on TE composites consisting of inorganic conductive fillers and organic polymer matrixes, which have become promising alternatives to inorganic thermoelectric materials.<sup>7,8</sup> A composite material is made by combining two or more materials—often ones that have very different properties. The different materials work together to give the composite unique properties.

The TE performance can be evaluated by the dimensionless figure of merit  $ZT$ , which is defined as  $ZT = S^2\sigma T/\kappa$ , where  $S$ ,  $\sigma$ ,  $\kappa$ , and  $T$  are the Seebeck coefficient, electrical conductivity, thermal conductivity, and absolute temperature, respectively. A high-performance thermoelectric material requires a high electrical conductivity, a high Seebeck coefficient, and a low thermal conductivity. However, there is a strong interdependence among these three parameters (e.g., increasing  $\sigma$  is usually accompanied by an increased  $\kappa$  and a decreased  $S$ ) which imposes restrictions on maximizing  $ZT$  in homogeneous bulk materials.<sup>9</sup> Thus, many researchers have sought to optimize the TE properties of composites by integrating the respective advantages of each thermoelectric component (e.g., polymer TE materials usually exhibit a low thermal conductivity and a relatively high Seebeck coefficient, and inorganic fillers generally possess high electrical conductivity).

Polymer TE materials, such as polyacetylene, polypyrroles, polyanilines, PTh, poly(3,4-ethylenedioxythiophene) and their related derivatives, have been widely studied due to their quite low thermal conductivity and high Seebeck coefficient as compared to inorganic materials.<sup>10,11</sup> Of these polymers, PTh has attracted great attention because of its low cost, easy synthesis, and relatively good environmental stability.<sup>12</sup> Among conventional inorganic TE materials, Bi<sub>2</sub>Te<sub>3</sub> is well-known as the best thermoelectric material<sup>13</sup> and has been used to prepare polymer-inorganic composite to obtain excellent TE performance.<sup>14</sup> Conductive fillers (e.g., G, carbon nanotube, and carbon black), especially G, is frequently applied in composites to achieve high electrical conductivity.<sup>15,16</sup> Hence, in this study, we fabricated a series of three-component composites consisting of PTh, Bi<sub>2</sub>Te<sub>3</sub> and G, with different proportions and compared their thermoelectric performance. In addition to conventional cold press molding described in literature,<sup>15</sup> an attempt was made to prepare Bi<sub>2</sub>Te<sub>3</sub>/G/PTh composite samples by SPS.

## EXPERIMENTAL PROCEDURE

Bi<sub>2</sub>Te<sub>3</sub> powders with a particle size of 30 nm were prepared by hydrothermal method according to the procedure previously reported by Ao et al.<sup>11</sup> PTh powder was synthesized by chemical oxidative polymerization of thiophene monomer with anhydrous iron (III) chloride in anhydrous chloroform, according to the method reported by Wang et al.<sup>17</sup> G, with particle sizes from 30  $\mu\text{m}$  to 50  $\mu\text{m}$ , was purchased from Nanjing Xianfeng Nano Technology

**Table I. Component proportions of Bi<sub>2</sub>Te<sub>3</sub>/Graphite/Polythiophene composites**

Serial number	Bi <sub>2</sub> Te <sub>3</sub> (wt.%)	G (wt.%)	PTh (wt.%)
A	5	40	55
B	10	40	50
C	5	75	20
D	10	70	20
S <sub>1</sub>	5	40	55
S <sub>2</sub>	5	75	20

Co., Ltd. Bi<sub>2</sub>Te<sub>3</sub>/G/PTh composite samples with different weight proportions (A, B, C, D, S<sub>1</sub> and S<sub>2</sub>), as shown in Table I, were mixed in 200 mL anhydrous ethanol by ultrasonication for 30 min and mechanical blending at 1500 rpm for an additional 30 min. Then the solvent was filtered and the residue sample was dried at 60°C for 24 h. The powder mixtures were milled for 1 h in an agate mortar and then the mixtures were milled in a 250 mL cylindrical steel jar (with five 10-mm diameter steel balls and ten 5-mm diameter steel balls inside) at a speed of 270 rpm for 10 h. Finally, the powers of A, B, C, and D samples were pressed into bulk composite materials at a specific pressure. We attempted to prepare the samples for measurements by using our previous reported method.<sup>18</sup> In order to confirm that the pressure we used to prepare samples has no big influence on the thermoelectric performance, we used small pressure differences (15 MPa and 20 MPa) for preparing samples of 5% Bi<sub>2</sub>Te<sub>3</sub>/40%G/PTh, and found that small pressure differences has limited effects on thermoelectric parameters of our composites (such as power factor and thermal conductivity), as shown in Table SI (Supporting Information). The cuboid specimen with dimensions of 16.0 mm  $\times$  5.10 mm  $\times$  3.0 mm was prepared under a pressure of 15 MPa for the electrical properties measurement, and the disk specimen with a diameter of 15.0 mm and a height of 3.0–4.0 mm was prepared under a pressure of 20 MPa for the thermal conductivity measurement.<sup>19</sup> The measurement was done in in-plane for disk specimens. All the prepared samples had close densities with the range from 1.56 g/cm<sup>3</sup> to 1.96 g/cm<sup>3</sup>, as shown in Table SII (Supporting Information). These samples were labelled as A, B, C and D, which were corresponding to their proportions. Besides, powders of S<sub>1</sub> and S<sub>2</sub> obtained by ball milling were used to prepare two additional bulk composite samples (labeled as S<sub>1</sub> and S<sub>2</sub>, respectively) by SPS, at 250°C for 5 min under a pressure of 40 MPa with a vacuum of  $1.5 \times 10^{-3}$ . A bar specimen with dimensions of 12.0 mm  $\times$  5.0 mm  $\times$  5.0 mm was prepared for electrical properties measurement in cross-plane, and a disk specimen with  $\Phi$ 12.7 mm  $\times$  2.0 mm was prepared for thermal conductivity measurement.

The phase structures of the composite samples were characterized by XRD on a Bruker D8 Advance x-ray diffractometer with Cu  $K\alpha$  radiation. Scanning electron microscopy (SEM, Hitachi S-4700) was used to observe the morphologies of the bulk samples. The thermal stability of the materials was examined by a thermo gravimetric analyzer (TGA-Q50, USA), which was conducted under a nitrogen flow of 40 mL min<sup>-1</sup>, from 50°C to 700°C at a heating rate of 10°C min<sup>-1</sup>. The electrical conductivities and Seebeck coefficients from 30°C to 120°C of the bulk samples were simultaneously measured by a Seebeck coefficient/electric conductivity measuring system (ZEM-2, ULVAC-RIKO, Japan) in a helium atmosphere. The thermal conductivity was measured via a thermal conductivity tester (KY-DRX-RW, Shanghai), as shown in Fig. S1 (Supporting Information). Finally, by interpolating the measurement data of  $S$ ,  $\sigma$  and  $\kappa$ , the figures of merit,  $ZT$ , at a given temperatures, for all the samples were calculated.

## RESULTS AND DISCUSSION

### XRD, SEM, and TGA Analysis of Bi<sub>2</sub>Te<sub>3</sub>/G/PTh Composites

Figure 1 shows the XRD patterns of pure PTh, Bi<sub>2</sub>Te<sub>3</sub> and Bi<sub>2</sub>Te<sub>3</sub>/G/PTh composites at room temperature. For the PTh powder, no obvious peaks can be observed from  $2\theta = 20^\circ$  to  $70^\circ$ , indicating an amorphous structure of PTh.<sup>20</sup> For the Bi<sub>2</sub>Te<sub>3</sub> powder, several peaks were observed and the sharp peak at  $2\theta = 28^\circ$  is a representative signal of the existence of Bi<sub>2</sub>Te<sub>3</sub>.<sup>11</sup> For the composites powders, the main diffraction peaks observed at  $2\theta = 26.5^\circ$  and  $2\theta = 55^\circ$  should be assigned to G,<sup>15</sup> and the representative peak at  $2\theta = 28^\circ$  was also observed for all the composites indicating that Bi<sub>2</sub>Te<sub>3</sub> powder was dispersed in G and PTh, though the low doping level of Bi<sub>2</sub>Te<sub>3</sub>.

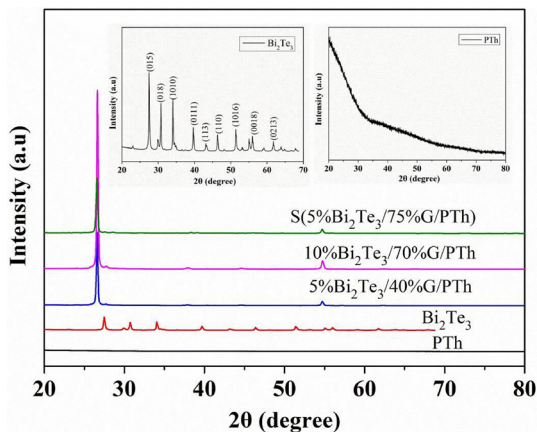


Fig. 1. X-ray diffraction patterns of PTh, Bi<sub>2</sub>Te<sub>3</sub>, and 5%Bi<sub>2</sub>Te<sub>3</sub>/40%G/PTh, 10% Bi<sub>2</sub>Te<sub>3</sub>/70%G/PTh, S(5%Bi<sub>2</sub>Te<sub>3</sub>/75%G/PTh) composites.

SEM images of pure PTh and Bi<sub>2</sub>Te<sub>3</sub> powders and the fracture surfaces of representative Bi<sub>2</sub>Te<sub>3</sub>/G/PTh composites are shown in Fig. 2. The Bi<sub>2</sub>Te<sub>3</sub> powders exhibit a granular-shaped and small-flake structure (Fig. 2a), and the PTh formed an irregular-shaped structure (Fig. 2b). The polymers and Bi<sub>2</sub>Te<sub>3</sub> were uniformly dispersed in the G matrix forming a flake-like structure as shown in Fig. 2c and d. It can be seen from the figure that the particles of Bi<sub>2</sub>Te<sub>3</sub>, PTh and G sheets are more tightly-joined shown in Fig. 2d than that shown in Fig. 2c, indicating that the structure of Bi<sub>2</sub>Te<sub>3</sub>/G/PTh composites become more dense after SPS, and PTh can act as an adhesive during the SPS process, which was further confirmed when comparing their densities. The density of 1.96 g/cm<sup>2</sup> of the sample prepared by SPS (S<sub>2</sub>) is larger than that of the sample prepared by cold pressing (C) with a density of 1.84 g/cm<sup>2</sup>. As shown in Table SII, the density of the samples became larger when increasing the amount of G, because the density of G is larger than that of the PTh. Samples prepared by SPS have slightly larger density compared to that of the samples prepared by cold pressing.

The TGA results of PTh, A, C and S<sub>2</sub> are shown in Fig. 3. PTh, A, C and S<sub>2</sub> suggested thermal stability below 200°C during the measurement time period (97 min) under ambient air. Dramatic weight loss was observed for pure PTh and its composites above 200°C, indicating the decomposition of PTh in the composites. The weight loss became slow and decreased as G content increased. The S<sub>2</sub> composite exhibited better thermal stability than any other materials, which should be attributed to the high thermal stability of G and the uniform dispersion of three components that can increase the thermal stability of the composites during the SPS process. These results indicate that the TE properties of the composites could be investigated below 200°C at which the polymer structure was undestroyed.

### Thermoelectric Properties of Bi<sub>2</sub>Te<sub>3</sub>/G/PTh Composites

The Seebeck coefficient ( $S$ ), electrical conductivity ( $\sigma$ ), power factor ( $P$ ), and thermal conductivity ( $\kappa$ ) for Bi<sub>2</sub>Te<sub>3</sub>/G/PTh composites are shown in Figs. 4, 5, 6, and 7, and Table II. As shown in Fig. 4, the Seebeck coefficient of Bi<sub>2</sub>Te<sub>3</sub>/G/PTh composites with different proportions keeps an almost constant range from 30°C to 60°C. It can be seen from Fig. 4 and Table II, the Seebeck coefficients of the composites decreased with increasing G content due to an increase in the carrier concentration;<sup>16</sup> this phenomena is consistent with the results report by Li et al.<sup>21</sup> As is illustrated in Table II, samples A and B with PTh content of about 50 wt.% exhibited much higher Seebeck coefficient values of 23.3 and 20.4  $\mu\text{V/K}$  than that of the G/50 wt.% PTh composite with a Seebeck coefficient value of 16.1 at 30°C, respectively.<sup>15</sup> These results clearly show that the



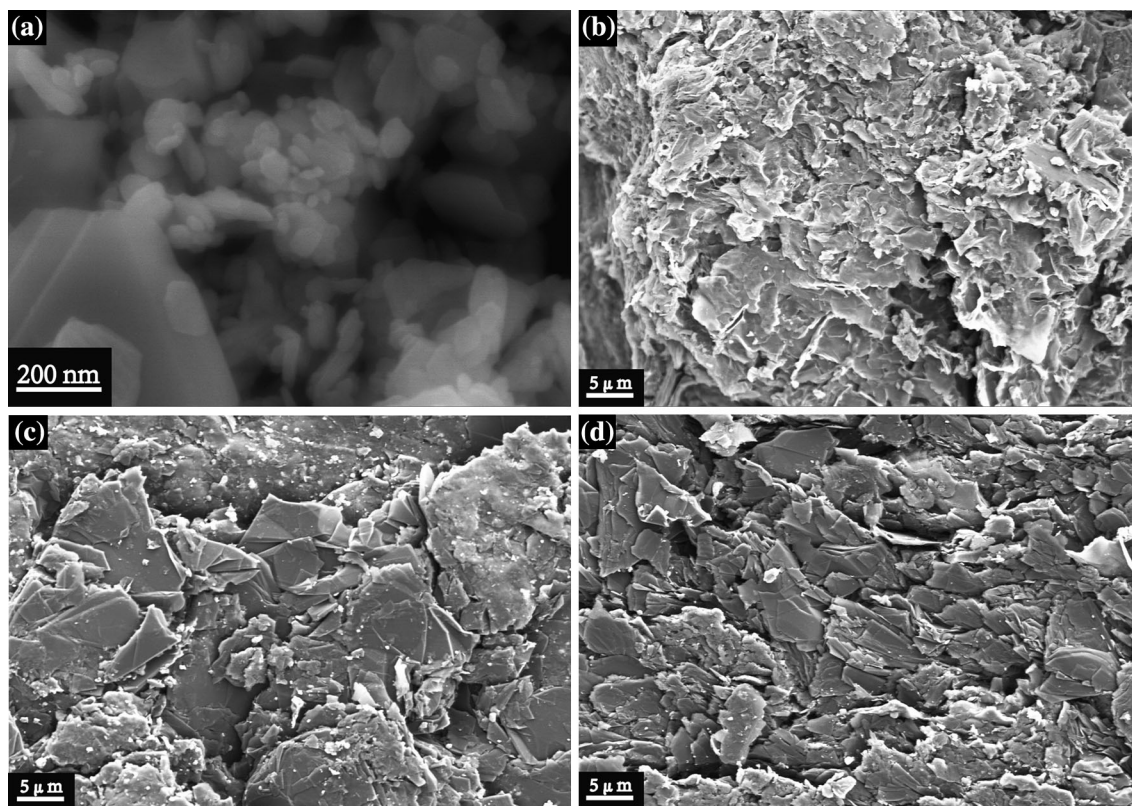


Fig. 2. SEM images of Bi<sub>2</sub>Te<sub>3</sub> (a), PTh (b), and 5%Bi<sub>2</sub>Te<sub>3</sub>/75%G/PTh (c), S(5% Bi<sub>2</sub>Te<sub>3</sub>/75%G/PTh) (d) composites.

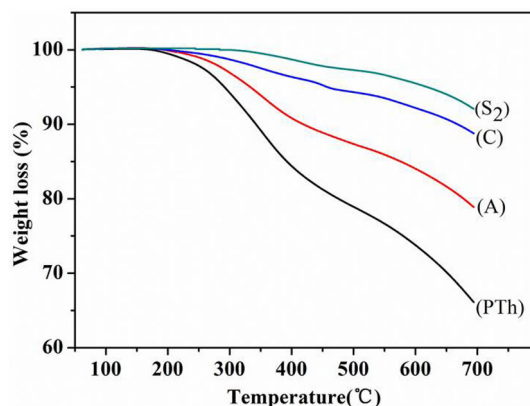


Fig. 3. TGA curves for PTh, and 5%Bi<sub>2</sub>Te<sub>3</sub>/40%G/PTh (A), 5% Bi<sub>2</sub>Te<sub>3</sub>/75%G/PTh (C), and S(5% Bi<sub>2</sub>Te<sub>3</sub>/75%G/PTh) (S<sub>2</sub>) composites.

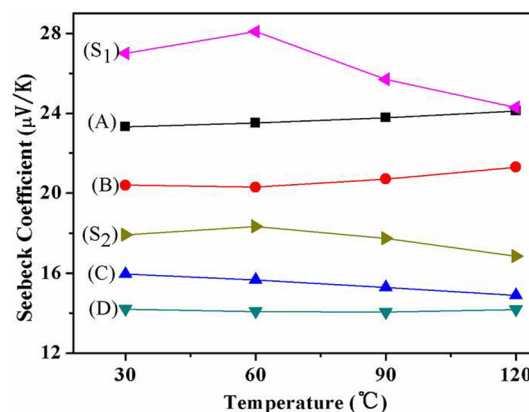


Fig. 4. Seebeck coefficient of these composites: (A) 5%Bi<sub>2</sub>Te<sub>3</sub>/40%G/PTh, (B) 10% Bi<sub>2</sub>Te<sub>3</sub>/40%G/PTh, (C) 5% Bi<sub>2</sub>Te<sub>3</sub>/75%G/PTh, (D) 10%Bi<sub>2</sub>Te<sub>3</sub>/70%G/PTh, (S<sub>1</sub>) S(5% Bi<sub>2</sub>Te<sub>3</sub>/40%G/PTh), (S<sub>2</sub>) S(5%Bi<sub>2</sub>Te<sub>3</sub>/75%G/PTh).

addition of Bi<sub>2</sub>Te<sub>3</sub> can greatly enhance the Seebeck coefficient values. The further addition of Bi<sub>2</sub>Te<sub>3</sub> in G/50 wt.% PTh composites from 5% to 10% slightly decreased the value of the Seebeck coefficient from 23.3 μV/K to 20.4 μV/K, which could be attributed to the lower number of interfaces formed between the fillers and matrix because of the higher density of Bi<sub>2</sub>Te<sub>3</sub> than that of G and PTh.<sup>18</sup> Similar results were also observed for composites C and D with PTh content of about 20 wt.%; they also exhibited much

higher Seebeck coefficient values of 15.9 μV/K and 14.2 μV/K than that of G/20 wt.% PTh composite 9.36 μV/K at 30°C.<sup>15</sup> These results also demonstrate that the addition of a small amount of Bi<sub>2</sub>Te<sub>3</sub> into Bi<sub>2</sub>Te<sub>3</sub>/G/PTh composites indeed increased the Seebeck coefficient of these composites. Composites S<sub>1</sub> and S<sub>2</sub>, which are prepared by the SPS process, exhibited a higher Seebeck coefficient compared to the composite A and C. One reason could be the samples prepared by SPS have larger densities

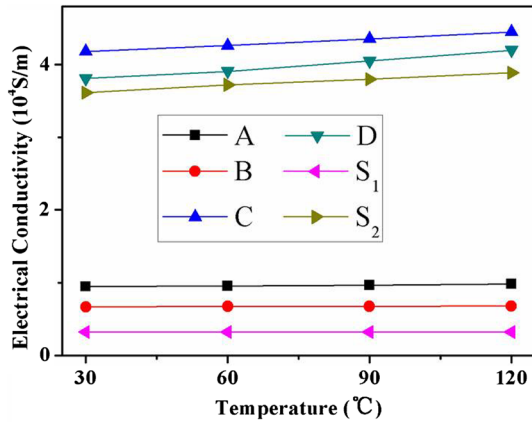


Fig. 5. Electrical conductivity of the composites: (A) 5%Bi<sub>2</sub>Te<sub>3</sub>/40%G/PTh, (B) 10% Bi<sub>2</sub>Te<sub>3</sub>/40%G/PTh, (C) 5% Bi<sub>2</sub>Te<sub>3</sub>/75%G/PTh, (D) 10%Bi<sub>2</sub>Te<sub>3</sub>/70%G/PTh, (S<sub>1</sub>) S(5% Bi<sub>2</sub>Te<sub>3</sub>/40%G/PTh), and (S<sub>2</sub>) S(5%Bi<sub>2</sub>Te<sub>3</sub>/75%G/PTh).

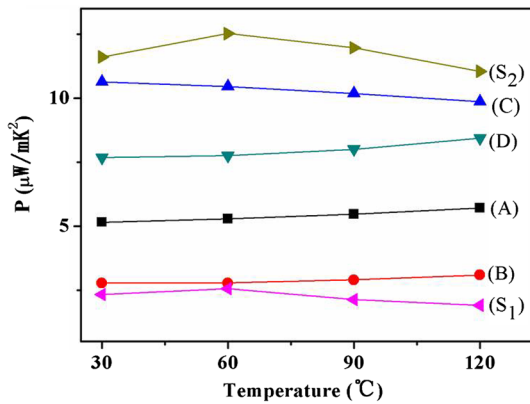


Fig. 6. Power factor of the composites: (A) 5%Bi<sub>2</sub>Te<sub>3</sub>/40%G/PTh, (B) 10% Bi<sub>2</sub>Te<sub>3</sub>/40%G/PTh, (C) 5% Bi<sub>2</sub>Te<sub>3</sub>/75%G/PTh, (D) 10%Bi<sub>2</sub>Te<sub>3</sub>/70%G/PTh, (S<sub>1</sub>) S(5% Bi<sub>2</sub>Te<sub>3</sub>/40%G/PTh), and (S<sub>2</sub>) S(5%Bi<sub>2</sub>Te<sub>3</sub>/75%G/PTh).

(Table III) and the other reason might be the PTh became softened during the SPS process, and the softened PTh were combined with both Bi<sub>2</sub>Te<sub>3</sub> and G more tightly under great pressure, which hindered the contact between Bi<sub>2</sub>Te<sub>3</sub> and G as a result.

The electrical conductivities of Bi<sub>2</sub>Te<sub>3</sub>/G/PTh composites are shown in Fig. 5 and Table II. The electrical conductivity of the composites dramatically increases with increasing G content. For example, the electrical conductivity of sample C with 75 wt.% G content is  $4.2 \times 10^4$  S/m at 30°C, which is about four times higher than that for sample A with 40 wt.% G content at the same temperature. The increased electrical conductivity with G content might be attributed to an increase in the carrier concentration and carrier mobility due to the excellent conductivity of G. The electrical conductivity of the samples prepared by SPS slightly decreased compared to the same samples prepared by cold pressing. For example, sample S<sub>2</sub> with 75 wt.% G content exhibits an electrical conductivity of

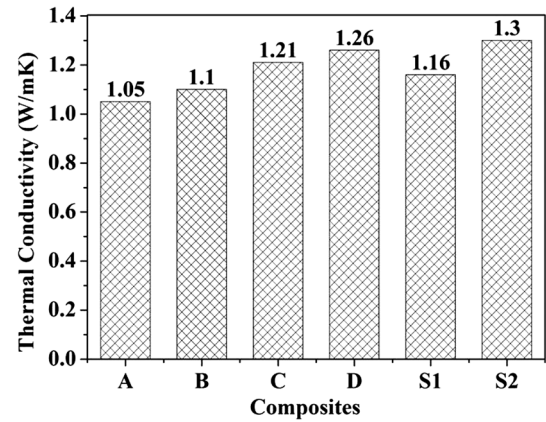


Fig. 7. Thermal conductivity of the composites: (A) 5%Bi<sub>2</sub>Te<sub>3</sub>/40%G/PTh, (B) 10% Bi<sub>2</sub>Te<sub>3</sub>/40%G/PTh, (C) 5% Bi<sub>2</sub>Te<sub>3</sub>/75%G/PTh, (D) 10%Bi<sub>2</sub>Te<sub>3</sub>/70%G/PTh, (S<sub>1</sub>) S(5% Bi<sub>2</sub>Te<sub>3</sub>/40%G/PTh), and (S<sub>2</sub>) S(5%Bi<sub>2</sub>Te<sub>3</sub>/75%G/PTh).

$3.6 \times 10^4$  S/m at 30°C, while the value for sample C is  $4.2 \times 10^4$  S/m. The slight decrease of electrical conductivity, probably due to the enhanced phase boundaries between the components, results from the high temperature and high pressure during the SPS process.<sup>11,22</sup> In addition, the electrical conductivity of the composites decreased with increasing Bi<sub>2</sub>Te<sub>3</sub> content, which results from the inherent poor conductivity of Bi<sub>2</sub>Te<sub>3</sub>.

The power factor ( $P$ ) for the Bi<sub>2</sub>Te<sub>3</sub>/G/PTh composites is shown in Fig. 6, which was calculated from the Seebeck coefficient  $S$  and the electrical conductivity  $\sigma$  ( $P = S^2\sigma$ ). The power factor ( $P$ ) for the composites increases dramatically with increasing G content due to a remarkable increase in electrical conductivity  $\sigma$ , and slightly decreases with increasing Bi<sub>2</sub>Te<sub>3</sub> content owing to a small decrease in  $\sigma$ . With a high doping level of G and the same proportions, the sample prepared by SPS exhibits a much higher power factor than that of the sample prepared by cold pressing, due to an enhanced Seebeck coefficient. The composite S<sub>2</sub> exhibits a power factor of  $11.62 \mu\text{W}/\text{mK}^2$  at 30°C, which is higher than that of sample C ( $10.65 \mu\text{W}/\text{mK}^2$  at 30°C), and higher than that of  $5.2 \pm 0.9 \mu\text{W}/\text{mK}^2$  reported by Xu et al.<sup>23</sup> However, the power factor of S<sub>1</sub>, which is  $2.33 \mu\text{W}/\text{mK}^2$  at 30°C, is much lower than that of sample A, due to a dramatically decreased electrical conductivity.

The thermal conductivity of Bi<sub>2</sub>Te<sub>3</sub>/G/PTh composites was measured using a KY-DRX-RW thermal conductivity tester, as shown in Fig. 7. According to the reported literatures,<sup>22,24</sup> the value of thermal conductivity of pure PTh and Bi<sub>2</sub>Te<sub>3</sub> is as low as 0.17 W/mK and 2.8 W/mK at room temperature, respectively, compared with G. From Fig. 7 we can see that the thermal conductivity of these composite samples increased with increasing Bi<sub>2</sub>Te<sub>3</sub> and G content, but remained at a low level, even at a high concentration of fillers. This should be attributed to the high interface density (the interfacial area per

**Table II. Effects of phase content on TE properties ( $S$ ,  $\sigma$ ,  $P$ ,  $\kappa$ ) at 30°C**

Samples	$S$ ( $\mu\text{V/K}$ )	$\sigma$ ( $\times 10^4$ S/m)	$P$ ( $\mu\text{W/mK}^2$ )	$\kappa$ (W/mK)
5% Bi <sub>2</sub> Te <sub>3</sub> /40%G/PTh (A)	23.3	0.95	5.1	1.05
10% Bi <sub>2</sub> Te <sub>3</sub> /40%G/PTh (B)	20.4	0.67	2.8	1.1
5% Bi <sub>2</sub> Te <sub>3</sub> /75%G/PTh (C)	15.9	4.2	10.6	1.21
10% Bi <sub>2</sub> Te <sub>3</sub> /70%G/PTh (D)	14.2	3.8	7.7	1.26
SPS(5% Bi <sub>2</sub> Te <sub>3</sub> /40%G/PTh) (S <sub>1</sub> )	27	0.32	2.3	1.16
SPS(5% Bi <sub>2</sub> Te <sub>3</sub> /75%G/PTh) (S <sub>2</sub> )	17.9	3.6	11.6	1.3

**Table III. Densities of samples prepared by different methods (cold-pressing versus SPS)**

Sample	Density (g/cm <sup>3</sup> )
5% Bi <sub>2</sub> Te <sub>3</sub> /40%G/PTh (A)	1.56
SPS(5% Bi <sub>2</sub> Te <sub>3</sub> /40%G/PTh) (S <sub>1</sub> )	1.62
5% Bi <sub>2</sub> Te <sub>3</sub> /75%G/PTh (C)	1.84
SPS(5% Bi <sub>2</sub> Te <sub>3</sub> /75%G/PTh) (S <sub>2</sub> )	1.96

unit volume) between Bi<sub>2</sub>Te<sub>3</sub> and G, because the thermal conductivity of polymer composite is dominated by the phonon-interface scattering, and a high interface density could also scatter phonons more effectively. Together with the low value of thermal conductivity of PTh, we can achieve the composite materials with a low thermal conductivity.<sup>9</sup>

### CONCLUSIONS

Bi<sub>2</sub>Te<sub>3</sub>/G/PTh composites with various proportions were successfully fabricated. The results demonstrate that the TE performance is simultaneously determined by three parameters (Seebeck coefficient  $S$ , electrical conductivity  $\sigma$ , and thermal conductivity  $\kappa$ ), of which the strong interdependence imposes restrictions on maximizing  $ZT$  in homogeneous bulk materials. A remarkable enhancement of electrical conductivity achieved by adding a high content of G can significantly improve the properties of Bi<sub>2</sub>Te<sub>3</sub>/G/PTh hybrid thermoelectric materials. The addition of low-content Bi<sub>2</sub>Te<sub>3</sub> can also increase the Seebeck coefficient to some extent and the process of SPS can increase the Seebeck coefficient while decreasing the electrical conductivity. From this work, we can conclude that the electrical conductivity, the Seebeck coefficient, and the thermal conductivity are not equal to the sum of the sub-components, but is a mixture between material architecture and microstructure. Further work on the improvement of the  $ZT$  value of the composites materials to realize a system application is ongoing in our group.

### ACKNOWLEDGEMENTS

The authors would like to thank the National Nature Science Foundation of China (Nos. 51003060

and 51171117) and the Shenzhen Sci & Tech Research Grant (JC20110 42100070A, ZYC201105 170225A) for their financial support.

### ELECTRONIC SUPPLEMENTARY MATERIAL

The online version of this article (doi: [10.1007/s11664-016-4663-6](https://doi.org/10.1007/s11664-016-4663-6)) contains supplementary material, which is available to authorized users.

### REFERENCES

- H. Ming, Q. Feng, and Z.Q. Lin, *Energy Environ. Sci.* 6, 1352 (2013).
- C. Han, Z. Li, and S.X. Dou, *Chin. Sci. Bull.* 59, 2073 (2014).
- A. Date, A. Date, C. Dixon, and A. Akbarzadeh, *Renew. Sustain. Energy Rev.* 33, 371 (2014).
- M. Hamid Elsheikh, D.A. Shnawah, M.F.M. Sabri, S.B.M. Said, M. Haji Hassan, M.B. Ali Bashir, and M. Mohamad, *Renew. Sustain. Energy Rev.* 30, 337 (2014).
- D.L. Zhao and G. Tan, *Appl. Therm. Eng.* 66, 15 (2014).
- M. Liebscher, T. Gärtner, L. Tzounis, M. Mičušík, P. Pötschke, M. Stamm, G. Heinrich, and B. Voit, *Compos. Sci. Technol.* 101, 133 (2014).
- J. Hyun, K. Myeongjin, and K. Jooheon, *J. Appl. Polym. Sci.* (2015). doi:[10.1002/app.42107](https://doi.org/10.1002/app.42107).
- H. Ju, M. Kim, and J. Kim, *J. Mater. Sci. Mater. Electron.* 26, 2544 (2015).
- M. He, J. Ge, Z.Q. Lin, X.H. Feng, X.W. Wang, H.B. Lu, Y.L. Yang, and F. Qiu, *Energy Environ. Sci.* 5, 8351 (2012).
- N. Dubey and M. Leclerc, *J. Polym. Sci. Polym. Phys.* 49, 467 (2011).
- W.Q. Ao, L. Wang, J.Q. Li, F. Pan, and C.N. Wu, *J. Electron. Mater.* 40, 2027 (2011).
- Y.J. Hu, H. Shi, H.J. Song, C.C. Liu, J.Q. Xu, L. Zhang, and Q.L. Jiang, *Synth. Met.* 181, 23 (2013).
- D.H. Kim and T. Mitani, *J. Alloy. Compd.* 399, 14 (2005).
- H. Pang, Y.Y. Piao, Y.Q. Tan, G.Y. Jiang, J.H. Wang, and Z.M. Li, *Mater. Lett.* 107, 150 (2013).
- J.J. Li, L. Wang, X.L. Jia, X.Z. Xiang, C.L. Ho, W.Y. Wong, and H. Li, *RSC Adv.* 4, 62096 (2014).
- S.A. Mansour, M. Hussein, and A.H. Moharram, *Adv Polym Technol* 33, 1 (2014).
- L. Wang, X.L. Jia, D.G. Wang, G.M. Zhu, and J.Q. Li, *Synth. Met.* 181, 79 (2013).
- J.J. Li, C.H. Lai, X.Z. Xiang, and L. Wang, *J. Mater. Chem. C* 3, 2693 (2015).
- C.H. Lai, J.J. Li, X.Z. Xiang, L. Wang, and D.Q. Liu, *Polym. Compos.* (2016). doi:[10.1002/pc.23913](https://doi.org/10.1002/pc.23913).
- M.R. Karim, C.J. Lee, and M.S. Lee, *J. Polym. Sci. Chem.* 44, 5283 (2006).

21. J. Li, C. Lai, X. Jia, L. Wang, X. Xiang, C.-L. Ho, H. Li, and W.-Y. Wong, *Compos. Part B* 77, 248 (2015).
22. Y. Du, K.F. Cai, S.Z. Shen, B.J. An, Z. Qin, and P.S. Casey, *J. Mater. Sci. Mater. Electron* 23, 870 (2012).
23. K.L. Xu, G.M. Chen, and D. Qiu, *J. Mater. Chem. A* 1, 12395 (2013).
24. B.Y. Lu, C.C. Liu, S. Lu, J.K. Xu, F.X. Jiang, Y.Z. Li, and Z. Zhang, *Chin. Phys. Lett.* 27, 1 (2010).